DOI: 10.1093/jnci/djq198
Advance Access publication on May 26, 2010.

ARTICLE

Effect of Noncompetitive Proteasome Inhibition on Bortezomib Resistance

Xiaoming Li, Tabitha E. Wood, Remco Sprangers, Gerrit Jansen, Niels E. Franke, Xinliang Mao, Xiaoming Wang, Yi Zhang, Sue Ellen Verbrugge, Hans Adomat, Zhi Hua Li, Suzanne Trudel, Christine Chen, Tomasz L. Religa, Nazir Jamal, Hans Messner, Jacqueline Cloos, David R. Rose, Ami Navon, Emma Guns, Robert A. Batey, Lewis E. Kay, Aaron D. Schimmer

Manuscript received June 29, 2008; revised April 27, 2010; accepted April 30, 2010.

Correspondence to: Aaron D. Schimmer, MD, PhD, 610 University Ave, Toronto, ON, Canada M5G 2M9 (e-mail: aaron.schimmer@utoronto.ca).

Background Bortezomib and the other proteasome inhibitors that are currently under clinical investigation bind to the catalytic sites of proteasomes and are competitive inhibitors. We hypothesized that proteasome inhibitors that act through a noncompetitive mechanism might overcome some forms of bortezomib resistance.

Methods 5-amino-8-hydroxyquinoline (5AHQ) was identified through a screen of a 27-compound chemical library based on the quinoline pharmacophore to identify proteasome inhibitors. Inhibition of proteasome activity by 5AHQ was tested by measuring 7-amino-4-methylcoumarin (AMC) release from the proteasome substrate Suc-LLVY-AMC in intact human and mouse leukemia and myeloma cells and in tumor cell protein extracts. Cytotoxicity was assessed in 5AHQ-treated cell lines and primary cells from myeloma and leukemia patients using AlamarBlue fluorescence and MTS assays, trypan blue staining, and annexin V staining. 5AHQ–proteasome interaction was assessed by nuclear magnetic resonance. 5AHQ efficacy was evaluated in three leukemia xenograft mouse models (9–10 mice per group per model). All statistical tests were two-sided.

Results 5AHQ inhibited the proteasome when added to cell extracts and intact cells (the mean concentration inhibiting 50% [IC_{50}] of AMC release in intact cells ranged from 0.57 to 5.03 μM), induced cell death in intact cells from leukemia and myeloma cell lines (mean IC_{50} values for cell growth ranged from 0.94 to 3.85 μM), and preferentially induced cell death in primary myeloma and leukemia cells compared with normal hematopoietic cells. 5AHQ was equally cytotoxic to human myelomonocytic THP1 cells and to THP1/BTZ500 cells, which are 237-fold more resistant to bortezomib than wild-type THP1 cells because of their overexpression and mutation of the bortezomib-binding β5 proteasome subunit (mean IC_{50} for cell death in the absence of bortezomib, wild-type THP1: 3.7 μM, 95% confidence interval = 3.4 to 4.0 μM; THP1/BTZ500: 6.6 μM, 95% confidence interval = 5.9 to 7.5 μM). 5AHQ interacted with the α subunits of the 20S proteasome at noncatalytic sites. Orally administered 5AHQ inhibited tumor growth in all three mouse models of leukemia without overt toxicity (eg, OCI-AML2 model, median tumor weight [interquartile range], 5AHQ vs control: 95.7 mg [61.4–163.5 mg] vs 247.2 mg [189.4–296.2 mg], $P = .002$).

Conclusions 5AHQ is a noncompetitive proteasome inhibitor that is cytotoxic to myeloma and leukemia cells in vitro and inhibits xenograft tumor growth in vivo. 5AHQ can overcome some forms of bortezomib resistance in vitro.

J Natl Cancer Inst 2010;102:1069–1082

The proteasomal degradation pathway rids cells of excess and misfolded proteins and regulates the cellular levels of proteins that are responsible for processes, such as cell cycle progression, DNA repair, and transcription [reviewed in (1)]. The proteasomal pathway of protein degradation is initiated by the sequential enzymatic activities of ubiquitin ligases E1, E2, and E3, which add chains of ubiquitin molecules onto the lysine residues of proteins to mark them for degradation [reviewed in (2,3)]. Ubiquitin-tagged proteins are degraded by the 26S proteasome, a multimeric enzyme complex consisting of α and β subunits located in the nucleus and cytoplasm. Chemical and peptidyl inhibitors of the proteasome prevent ubiquitin-mediated protein degradation. In vitro and in vivo studies demonstrate that proteasome inhibitors induce cell death in malignant cells and inhibit tumor growth in mouse models of malignancy (4), thus supporting the development of proteasome inhibitors as therapeutic agents for the treatment of malignancies.

All chemical proteasome inhibitors currently approved or under clinical evaluation, such as bortezomib and NPI-0052, bind threonine residues in the active sites of the β subunits of the 20S proteasome (the core complex of the 26S proteasome in eukaryotes, which degrades ubiquitinated target molecules in an

CONTEXT AND CAVEATS

Prior knowledge

Proteasome inhibitors that are currently approved or under clinical investigation, including bortezomib, bind to the catalytic sites of proteasomes and are competitive inhibitors. Proteasome inhibitors that act through a noncompetitive mechanism might overcome some forms of bortezomib resistance.

Study design

Screening of a 27-compound chemical library based on the quinoline pharmacophore identified 5-amino-8-hydroxyquinoline (5AHQ) as a proteasome inhibitor. The mechanism of inhibition was examined in isolated proteasomes. The effects of 5AHQ on proteasome inhibition and on cell viability and apoptosis were tested in leukemia and myeloma cell lines and in primary cells from myeloma and leukemia patients. 5AHQ efficacy was evaluated in three leukemia xenograft mouse models.

Contribution

5AHQ bound to the α subunits of the 20S proteasome at noncatalytic sites. 5AHQ inhibited the proteasome and induced cell death in leukemia and myeloma cell lines and preferentially induced cell death in primary myeloma and leukemia cells compared with normal hematopoietic cells. 5AHQ was equally cytotoxic to a bortezomib-resistant myeloma cell line and the parental cell line from which it was derived. Orally administered 5AHQ inhibited tumor growth in all three mouse models of leukemia without overt toxicity.

Implications

5AHQ may represent a new strategy for proteasome inhibition in cancer cells and a potential lead for a new class of therapeutic agents.

Limitations

The possibilities that 5AHQ simultaneously binds to α and β subunits, that a 5AHQ metabolite is primarily responsible for proteasome inhibition, and that 5AHQ or a metabolite also inhibits the proteasome through indirect effects were not excluded. 5AHQ may have additional targets beyond the proteasome, and inhibition of these other targets may also contribute to its anticancer effects.

From the Editors

ATP-dependent manner), thereby competitively inhibiting the enzymatic activity of the proteasome (5–7). In clinical trials, the proteasome inhibitor bortezomib has demonstrated clinical efficacy in patients with new diagnosed and relapsed multiple myeloma and mantle cell lymphoma (8,9). However, most patients who are treated with this drug alone do not achieve complete remission, and the majority of responders ultimately relapse (8,9). Several mechanisms of resistance to bortezomib have been identified (10), including mutation and overexpression of the β5 subunit of the proteasome to which bortezomib binds (11). Molecules that inhibit the proteasome through a mechanism distinct from that of bortezomib could be useful for overcoming some forms of resistance to this drug or used in combination with bortezomib to improve clinical outcomes.

Previously, we demonstrated inhibition of the proteasome by chloroquine and clioquinol, compounds that share a common quinoline pharmacophore (12,13). Chloroquine binds the α subunits of the proteasome and inhibits the enzyme noncompetitively (13). However, because supra-pharmacological concentrations of chloroquine are required to observe these effects, we could not investigate the effects of chloroquine on proteasomal function in intact cells alone or in combination with bortezomib. Clioquinol is more active than chloroquine, but its poor solubility in water precludes detailed mechanistic studies. Therefore, we screened a library of chemical compounds that were based on the quinoline pharmacophore to identify proteasome inhibitors that may be more amenable than chloroquine and clioquinol for in vitro and in vivo studies. Here, we characterize 5-amino-8-hydroxyquinoline (5AHQ), the most potent inhibitor identified in this screen in vitro and in mouse xenograft models.

Materials and Methods

Cell Lines

Human multiple myeloma KMH11, KMS18, LP1, My5, and UTMC2 cells (14), whose identities were confirmed by cytogenetic profiling, were grown in Iscove modified Dulbecco's medium (Ontario Cancer Institute, Toronto, ON, Canada). Human OCI-AML2, NB4, KG1A (14), and K562 (American Type Culture Collection, Manassas, VA) and murine MDAY-D2 (15) leukemia cell lines, whose identities were verified by gene expression profiling, were maintained in RPMI-1640 medium (Ontario Cancer Institute). Human myelomonocytic THP1 cells and the bortezomib-resistant derivative cell lines THP1/BTZ50, THP1/BTZ100, THP1/BTZ200, and THP1/BTZ500 (11) were grown in RPMI-1640 medium supplemented with 20 mM HEPES and 2 mM glutamine; THP1/BTZ50, THP1/BTZ100, THP1/BTZ200, and THP1/BTZ500 were grown in the presence of 50, 100, 200, and 500 nM bortezomib, respectively (Millennium Pharmaceutics, Cambridge, MA). Bortezomib-resistant THP1 cells were maintained in medium containing bortezomib for at least 3 days before their use in an experiment. All media were supplemented with 10% fetal calf serum, 100 μg/mL penicillin, and 100 U/mL streptomycin (all from Hyclone, Logan, UT).

Primary Cells

Primary human acute myeloid leukemia (AML) and chronic lymphocytic leukemia (CLL) cells were isolated by Ficoll (Sigma-Aldrich, St Louis, MO) density gradient centrifugation from peripheral blood samples obtained from AML (n = 4) and CLL (n = 5) patients, respectively, attending the Princess Margaret Hospital (Toronto, ON, Canada) for whom at least 80% of the mononuclear cells in their peripheral blood were malignant. Bone marrow aspirates were obtained from patients with multiple myeloma (n = 3) attending the Princess Margaret Hospital. Primary normal hematopoietic cells were obtained from healthy volunteers (n = 4) donating peripheral blood stem cells (PBSCs) for allotransplantation. Mononuclear cells were isolated by Ficoll density centrifugation. Primary cells were cultured at 37°C in Iscove modified Dulbecco's medium supplemented with 10% fetal calf serum, 1 mM L-glutamine, 100 μg/mL penicillin, and 100 U/mL streptomycin. All patients and healthy volunteers provided written informed consent. The collection and use of human tissue for this

study were approved by the local ethics review board (University Health Network, Toronto, ON, Canada).

Assessment of Proteasome Enzymatic Activity

To assess the effects of 5AHQ on the enzymatic activity of the proteasome in vitro, cellular proteins were extracted from myeloma UTMC2, KMH11, and KMS18 cells and from leukemia OCI-AML2, NB4, KG1A, MDAY-D2, and K562 cells with lysis buffer (50 mM HEPES [pH 7.5], 150 mM NaCl, 1% Triton X-100, and 2 mM ATP). For each assay, 2 μg of protein was incubated for 2 hours at 37°C with increasing concentrations of 5AHQ (Sigma-Aldrich) diluted in assay buffer (50 mM Tris–HCl [pH 7.5] and 150 mM NaCl). After incubation, the fluorogenic proteasome substrate *N*-Succinyl-Leu-Leu-Val-Tyr-AMC (7-amino-4-methylcoumarin) (Suc-LLVY-AMC; BIOMOL International, Plymouth Meeting, PA) was added to each reaction at a final concentration of 40 μM and the amount of free AMC released was measured with the use of a fluorescent spectrophotometric plate reader at excitation and emission wavelengths of 380 and 460 nm, respectively. Experiments were performed at least in duplicate and repeated at least twice (n = 4–12 data points).

To assess the effects of 5AHQ on the enzymatic activity of the proteasome in intact cells, leukemia OCI-AML2, NB4, KG1A, and MDAY-D2 cells and myeloma UTMC2, KMH11, KMS18, and MY5 cells were incubated with increasing concentrations of 5AHQ for 22 hours at 37°C. The cells were lysed in lysis buffer. For each assay, Suc-LLVY-AMC was added to 2 μg of protein and the generation of free AMC was measured over time with the use of a fluorescent spectrophotometric plate reader as described above. Experiments were performed at least in duplicate and repeated at least twice.

To assess the effects of 5AHQ on the enzymatic activity of purified proteasomes, we isolated proteasome complexes from rabbit muscle and from *Thermoplasma acidophilum* as described previously (13,16). Briefly, *Escherichia coli* BL21-CodonPlus(DE3) cells (Stratagene, Wilmington, DE) expressing the *T acidophilum* α and β proteasome subunits were grown in lysogeny broth (10 g tryptone, 5 g yeast extract, and 10 g NaCl in 1 L water, pH 7.4). Protein was purified on nickel–nitriloacetic acid (Ni-NTA) resin (Qiagen, Mississauga, ON, Canada), followed by cleavage of an amino-terminal hexa-His purification tag on the α subunit using tobacco etch virus (TEV) protease that was purified from *E coli* carrying a plasmid that overexpresses the His-tagged protease (13) followed by gel filtration. The proteasome is spontaneously formed in the *E coli* cells from the α and β subunits. The proteasome consisting of α subunits and lacking the β subunits, also called the half-proteasome, was produced by overexpressing the α subunits that carried a TEV-cleavable His tag in *E coli* BL21-CodonPlus(DE3) cells. Purification of the half-proteasome was performed as above.

Methyl labeling of the proteasome subunits for nuclear magnetic resonance (NMR) analysis was achieved by growing *E coli* BL21-CodonPlus(DE3) cells in D_2O-based minimal medium with ^{2}H- and ^{12}C-labeled glucose as the carbon source. One hour before induction of protein expression with isopropyl β-D-1-thiogalactopyranoside, *E coli* were treated with α-ketobutyric acid (60 mg/L; one methyl group labeled with $^{13}CH_3$, and the other was labeled with $^{12}CD_3$) and α-ketoisovaleric acid (one methyl group labeled with $^{13}CH_3$; 100 mg/L; both from Sigma-Aldrich). These precursor molecules are metabolized by the *E coli* cells, resulting in labeling of methyl groups with $^{13}CH_3$ in the Ile, Leu, and Val residues in an otherwise fully deuterated 12-carbon–labeled protein (17). Proteins were purified by Ni-NTA affinity resin and size exclusion chromatography.

Rabbit proteasomes were isolated from homogenates of the psoas muscles from Zealand white male rabbits that were centrifuged (100 000*g*) and applied to a 100-mL DE52 column. Bound protein was eluted, concentrated, dialyzed, and applied to a Mono Q column (Amersham Pharmacia, Piscataway, NJ). Bound protein was eluted, concentrated, and applied to a Superose 6 gel filtration column (Amersham Pharmacia). Fractions were collected, and the active fractions (those that released AMC from Suc-LLVY-AMC) were pooled, dialyzed, and applied to a DEAE Affi-Gel Blue column (Sigma-Aldrich). Active fractions were then collected and pooled for use in subsequent experiments.

Increasing concentrations of 5AHQ (0, 1.25, 2.5, 5, and 10 μM), MG132 (0, 0.078, 0.156, 0.312, 0.625, and 1.25 μM; BIOMOL International), and bortezomib (0, 2.5, 5, and 10 nM) were added to isolated rabbit proteasomes in 50 mM HEPES (pH 7.5), 1 mM dithiothreitol, and 0.018% sodium dodecyl sulfate (SDS) (18) and to purified *T acidophilum* proteasomes in 50 mM Tris–HCl (pH 7.5) and 150 mM NaCl (13). After 1 hour of incubation at 37°C, the AMC-conjugated proteasomal substrate benzyloxycarbonyl-L-leucyl-L-leucyl-L-glutamyl-methylcoumarylamide (Z-LLE-AMC; BIOMOL International) was added at final concentrations of 500, 250, 125, 62.5, and 31.25 μM, and the rate of free AMC release was measured over time with the use of a fluorescent spectrophotometric plate reader as described above. The kinetics by which 5AHQ and MG132 inhibited purified proteasome was determined using SigmaPlot software 11.0 and Enzyme Kinetics 1.3 (both from Systat Software, San Jose, CA).

Identification of 5AHQ

We compiled a chemical library of 27 compounds (all from Sigma) that were based on the quinoline pharmacophore and included various halogenated and alkyl-substituted quinolines, hydroxyquinolines, and quinoline hydrazones because we have previously shown that quinoline compounds can inhibit the proteasome (13). Aliquots of this library (final concentration of 3.9 μM) were added to 2 μg of whole-cell extract from MDAY-D2 leukemia cell line in reaction buffer (same as described above). After incubation for 2 hours at 37°C, the fluorogenic proteasome substrate Suc-LLVY-AMC (final concentration 40 μM) was added to each reaction. The amount of free AMC released was measured with the use of a fluorescent spectrophotometric plate reader at excitation and emission wavelengths of 380 and 460 nm, respectively, as described above.

NMR Assessment of Inhibitor Binding to the Proteasome

NMR experiments with the α_7-α_7 half-proteasome were performed on a 600-MHz spectrometer (Varian, Palo Alto, CA) at 50°C using samples that contained approximately 4 μM of proteasome (approximately 50 μM of α-monomer), 100% D_2O, 25 mM potassium phosphate (pH 6.8), 50 mM NaCl, 1 mM EDTA, 0.03% NaN_3, and 2 mM dithiothreitol, similar to that previously described (16,19).

NMR data were processed and analyzed with the nmrPipe/nmrDraw software package (20).

Cell Viability and Apoptosis Assays

The viability of leukemia and myeloma cells treated with 5AHQ or bortezomib was assessed with the use of a CellTiter 96 AQueous One Solution Cell Proliferation Assay (Promega, Madison, WI), which is a form of the 3-(4,5-dimethylthiazol-2-yl)-5-(3-carboxymethoxyphenyl)-2-(4-sulfophenyl)-2*H*-tetrazolium inner salt (MTS) assay, or with fluorescence-based AlamarBlue cell viability reagent (Invitrogen, Carlsbad, CA) according to manufacturer's instructions and as described previously (21,22) or by trypan blue staining. Apoptosis was measured by staining cells treated with 5AHQ with annexin V–fluorescein isothiocyanate and propidium iodide (both from Biovision Research Products, Mountain View, CA) and flow cytometry according to manufacturer's instructions and as previously described (23). Experiments were performed at least in duplicate and repeated at least twice (n = 4–20 data points). Viable primary myeloma cells were identified by staining with phycoerythrin-conjugated mouse monoclonal anti-CD138 antibody (20 μL/10^6 cells; Beckman Coulter, Brea, CA). The percentage of myeloma cells that were CD138 positive and annexin V negative after 5AHQ treatment compared with untreated samples was quantified as a marker of cell viability as previously described (24).

Mouse Xenograft Models

Mouse MDAY-D2 leukemia cells (5×10^5 cells per mouse) were injected intraperitoneally into sublethally irradiated (3.5 Gy) 5- to 6-week-old male and female nonobese diabetic/severe combined immunodeficient (NOD/SCID) mice (Ontario Cancer Institute). Beginning the next day, the mice were treated by oral gavage with 5AHQ at 50 mg/kg body weight in 0.4% Tween 80 in phosphate-buffered saline (vehicle) or vehicle control once per day for 8 days, a duration of treatment that was based on previous experiments to permit evaluation of differences in tumor size without causing distress to the mouse (data not shown) (n = 10 mice per group [five male and five female]). The number of mice per group was selected based on the numbers that could be managed effectively during the experiment. Mice were killed by CO_2 inhalation, and the weight and volume of the single intraperitoneal tumor that developed in each mouse were measured.

Human leukemia K562 (3×10^6) or OCI-AML2 (2×10^6) cells were injected subcutaneously into one flank of sublethally irradiated 5- to 6-week-old male and female NOD/SCID mice. When tumors were palpable (approximately 1 week after injection), the mice were treated with 5AHQ (50 mg/kg body weight) in vehicle or vehicle control by oral gavage once daily for 10 days (n = 10 mice per group for K562 [five male and five female] and n = 9 per group for OCI-AML2 [four male and five female]). The number of mice per group was selected based on the numbers that could be managed effectively during the experiment. The duration of treatment was based on previous experiments to permit evaluation of differences in tumor size without causing distress to the mouse (data not shown). Mice were killed by CO_2 inhalation, and their tumors were weighed.

To assess the effect of 5AHQ on the enzymatic activity of the proteasome in tumors, the leukemia xenograft tumors harvested from mice bearing subcutaneous OCI-AML2 tumors from the experiment described above were disaggregated to produce a single-cell suspension in phosphate-buffered saline by grinding the tumor with a 3-mL plunger of a syringe while the tumor was on top of a 40-μm nylon cell strainer (BD Biosciences, San Jose, CA). The resulting cells were lysed in lysis buffer, and the enzymatic activity of the proteasome was determined as described above.

Mouse studies were carried out according to the regulations of the Canadian Council on Animal Care and with the approval of the local ethics review board.

Immunoblotting

Whole-cell lysates were prepared from untreated MY5 (myeloma) and OCI-AML2 and K562 (leukemia) cells, as described previously (21). Whole-cell lysates were also prepared from myeloma LP1 cells treated for 24 hours with 2.5, 5, or 10 μM 5AHQ or buffer control. Briefly, 1×10^6 cells were washed with phosphate-buffered saline and resuspended in immunoblot lysis buffer (10 mM Tris [pH 7.4], 150 mM NaCl, 0.1% Triton X-100, 0.5% sodium deoxycholate, and 5 mM EDTA) containing Complete Protease Inhibitor cocktail tablets (Roche, Indianapolis, IN). Protein concentrations were determined by the Bradford assay. Equal amounts of protein were resolved on to SDS–polyacrylamide gels followed by transfer to nitrocellulose membranes. Membranes were incubated with a rabbit polyclonal anti-human ubiquitin antibody (1:1000 dilution; Calbiochem, San Diego, CA), a rabbit polyclonal anti-human β 5 subunit antibody (1:1000 dilution; BIOMOL International), a mouse monoclonal anti-human α 7 subunit antibody (1:1000 dilution; BIOMOL International), or a mouse monoclonal anti-β-actin antibody (1:10000 dilution; Sigma-Aldrich), followed by incubation with horseradish peroxidase–conjugated goat anti-mouse or anti-rabbit IgG (each at 1:3000 dilution; Amersham Bioscience UK, Little Chalfont, UK). Antibody binding was detected by use of the enhanced chemical luminescence method (Pierce, Rockford, IL).

Enzyme-Linked Immunosorbent Assay of NF-Kappa B Activity

NF-Kappa B activity was measured with the use of a Trans-AM NF-Kappa B p65 transcription factor assay kit (Active Motif, Carlsbad, CA) according to the manufacturer's instructions. Briefly, 3.2×10^6 MDAY-D2 cells were treated with increasing concentrations of 5AHQ for 24 hours. Cells were then treated with tumor necrosis factor alpha (TNF-α; 10 nM) or buffer control (RPMI-1640) for 1 hour before harvesting. Nuclear extracts were prepared by using a Nuclear Extract kit (Active Motif) according to the manufacturer's instructions. An enzyme-linked immunosorbent assay with a chemiluminescence readout was used to measure binding of the NF-Kappa B transcription factor subunit p65 to a DNA consensus sequence (5′-GGGACTTTCC-3′) cross-linked to 96-well plates. Experiments were performed in triplicate and repeated three times (n = 9 data points).

Pharmacokinetic Studies

To partially characterize the pharmacokinetics of 5AHQ, sublethally irradiated NOD/SCID mice were injected subcutaneously

in one flank with 1×10^6 MDAY-D2 cells. Seven days after tumor cell injection, when palpable tumors had formed, mice were treated once with 5AHQ (50 mg/kg body weight) by oral gavage, and at increasing times after treatment, mice were killed by CO_2 inhalation, and their blood and tumors were harvested, frozen on dry ice, and stored at −70°C (n = 3 mice per time point; n = 27 mice total). Plasma was isolated from the whole blood and frozen on dry ice and stored at −70°C. Plasma samples were thawed on ice; 10 µL of 4 µg/mL 5-fluoro-2′-deoxyuridine (internal standard) and 10 µL of 2 M HCl and 100 mM sodium bisulfite were added to a 25 µL sample of plasma, followed by addition of 75 µL of acetonitrile. The samples were mixed by vortexing and centrifuged at 15 000*g* for 5 minutes. The supernatant was collected, dried in a SpeedVac (Savant/Thermo, Waltham, MA), and reconstituted in 50 µL of 5 mM HCl and 2 mM dithiothreitol. Frozen tumor samples were weighed, two volume equivalents of water were added, and the tumor was homogenized with the use of a Powergen 125 homogenizer (Fischer, Ottawa, Canada). The homogenates were stored at −70°C.

Levels of 5AHQ in the mouse plasma and tumor homogenates were determined by liquid chromatography–mass spectrometry analysis using an Acquity UltraPerformance Liquid Chromatography System coupled to an eLambda PDA detector in line with a Quattro Premier mass spectrometer (all from Waters, Milford, MA). A BEH C18 column (2.1 × 100 mm, 1.7 µm; Waters) was used for separations with the following elution gradient: 0.2 minutes 2% B, 4.2 minutes 40% B, and 4.4 minutes 100% B, where A is 0.1% formic acid in water and B is methanol. A methanol flush and re-equilibration following the gradient resulted in a final run time of 8 minutes. The mass spectrometry instrument was operated in ES+ mode at unit resolution with 3.5 kV capillary voltage, source and desolvation temperatures of 120°C and 350°C, respectively, cone and desolvation N_2 gas flows of 50 and 1000 L/hour, respectively, and an Argon collision gas pressure of 5.1 mbar.

Calibration was carried out using 5AHQ standards that ranged from 0.01 to 4 µg/mL, each containing 5-fluoro-2′-deoxyuridine internal standards at 0.8 µg/mL. An additional series of standards comprising the oxidized form of 5AHQ was also used to quantify this metabolite. The *m/z* of 5AHQ was 161, and the *m/z* of the oxidized form was 162. The ultraviolet–visible spectra produced a spectral pattern similar to the mass spectrometry spectra. The m/z of the amino-linked glucuronide of 5AHQ was predicted based on a peak mass *m/z* of 337 (adduct mass of 176, glucuronic acid minus H_2O), a primary fragment *m/z* of 161, and a ultraviolet–visible spectrum similar to that of 5AHQ. Retention times for glucuronidated 5AHQ, 5AHQ, oxidized 5AHQ, and 5-fluoro-2′-deoxyuridine were 1.9, 2, 2.6, and 3.2 minutes, respectively.

Phamacokinetic analysis was carried out using Phoenix WinNonlin software version 1.0.0 (Pharsight, St Louis, MO).

Toxicology Studies

Studies to evaluate the toxicity of 5AHQ were performed by ChemPartners (Shanghai, China). CD1 mice (n = 5 mice of each sex per treatment group; ChemPartners) were treated with 5AHQ at 0 (control), 100, 200, or 300 mg/kg body weight/d by oral gavage for 14 days. An additional five mice of each sex were assigned to the control and 300-mg/kg dose groups for a recovery during which mice did not receive 5AHQ for a 1-week period after the 14-day treatment with 5AHQ. In the high-dose group, the dose of 5AHQ was increased to 450 mg/kg body weight/d starting on day 10 because of a lack of overt toxicity. Body weight, food consumption, behavior, and appearance were measured over time. Mice were weighed to record their body weight. Changes in the weight of food in the cage were recorded as a measure of food consumption. Mice were observed daily for physical abnormalities and abnormal behavior. At the end of the treatment and recovery periods, mice were killed by CO_2 inhalation, their blood sent for chemistry and hematology analysis, and their organs were examined for signs of gross toxicity.

Statistical Analysis

Data are presented as mean values with 95% confidence intervals (CIs) unless otherwise indicated. For in vivo studies, the Mann–Whitney rank sum nonparametric method was used to test for differences between treatment groups in the weight of the tumors. The *t* test was used for comparisons of two groups in the in vitro studies. All statistical tests were two-sided, and a *P* value less than .05 was considered statistically significant.

The kinetics by which 5AHQ and MG132 inhibited proteasomes purified from rabbit muscle were determined using SigmaPlot 11.0 and Enzyme Kinetics 1.3 software (both from Systat Software). Isobologram analysis to evaluate the combination of 5AHQ and bortezomib on cell viability and the enzymatic activity of the proteasome was performed with CalcuSyn software (Biosoft, Ferguson, MO, and Cambridge, UK), in which a combination index (CIN) less than 0.9 indicates synergism, a CIN greater than 1.1 indicates antagonism, and a CIN of 0.9–1.1 indicates additivity (25).

Results

Effect of 5AHQ on the Proteasome

Novel inhibitors of the proteasome might be useful probes to understand this enzymatic complex and leads for therapeutic agents that can overcome resistance to existing proteasome inhibitors, such as bortezomib. We screened a chemical library of compounds that were based on the quinoline pharmacophore and included various halogenated and alkyl-substituted quinolines, hydroxyquinolines, and quinoline hydrazones for compounds that inhibited the enzyme activity of the proteasome when added to protein extracts from malignant cells. The most potent chemical inhibitor of the proteasome identified in this screen was 5AHQ (Figure 1). When added to protein extracts derived from mouse leukemia MDAY-D2 cells, 5AHQ inhibited the enzymatic activity of the proteasome at low micromolar concentrations (0 vs 3.9 µM 5AHQ, mean relative residual proteasome activity = 100% vs 48.3%, difference = 51.7%, 95% CI = 50.2% to 53.2%; $P < .001$ [*t* test]). 5AHQ had similar inhibitory effects on proteasome activity when it was added to protein extracts derived from a panel of human leukemia and myeloma cell lines (Table 1) (mean IC_{50} for proteasome inhibition, defined as the concentration that caused 50% inhibition of AMC release, OCI-AML2: 4.2 µM, 95% CI = 3.61 to 4.79 µM; NB4: 2.4 µM, 95% CI = 2.22 to 2.58 µM; KG1A: 5.3 µM, 95% CI = 4.53 to 6.07 µM; MDAY-D2: 2.64 µM, 95%

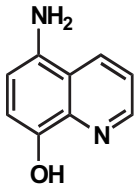

5AHQ
(5-amino-8-hydroxyquinoline)

Figure 1. Chemical structure of 5-amino-8-hydroxyquinoline (5AHQ).

CI = 2.17 to 3.11 μM; UTMC2: 2.54 μM, 95% CI = 2.34 to 2.74 μM; KMH11: 1.32 μM, 95% CI = 0.94 to 1.70 μM; KMS18: 0.57 μM, 95% CI = 0.56 to 0.58 μM).

Mechanism of 5AHQ Inhibition

To investigate the mechanism by which 5AHQ inhibits the proteasome, we conducted detailed enzymatic studies using purified proteasomes isolated from rabbit muscle. By Lineweaver–Burk plot analysis, 5AHQ inhibited the rabbit proteasome with a mean K_i of 2.1 μM (95% CI = 2.08 to 2.33 μM). The pattern of inhibition fits best to a noncompetitive model (sum of squares = 0.531, Akaike's information criterion (AICc) = −121.679, Sy.x [SD of the vertical distance of the point from the line] = 0.135) (Figure 2, A and Supplementary Figure 1, A [available online]). Notably, a plot of the enzyme activity vs the inhibitor concentration did not fit well to competitive (sum of squares = 1.897, AICc = −80.927, Sy.x = 0.256) or uncompetitive (sum of squares = 4.597, AICc = −52.609, Sy.x = 0.398) models of inhibition (Figure 2, A, inset, and data not shown, respectively). 5AHQ also inhibited a recombinant proteasome from the archaebacterium *T acidophilum* with noncompetitive kinetics (Supplementary Figure 2, available online). However, 5AHQ was a less potent inhibitor of the archaebacterial proteasome, with a mean K_i of 161 μM (95% CI = 153 to 169.6 μM), which may reflect small differences in the binding pocket for the inhibitor between the archaebacterial and eukaryotic proteasomes (26,27). By contrast, the proteasome inhibitor MG132, which binds the active site of the proteasome, inhibited the rabbit proteasome competitively, as described previously (13) (Figure 2, B and Supplemental Figure 1, A [available online]). Thus, 5AHQ inhibits the proteasome through a mechanism distinct from that of MG132.

Combined Effect of 5AHQ and Bortezomib on Proteasome Activity

Given that 5AHQ inhibited the proteasome through a mechanism distinct from competitive proteasome inhibitors such as MG132 [Figure 2; (12)] and bortezomib (7), we evaluated the effect of the combination of 5AHQ and bortezomib on the proteasome using isobologram analyses. 5AHQ acted synergistically with bortezomib to produce greater proteasome inhibition than was observed either agent alone, with CIN values of 0.46, 0.63, and 0.86 at the concentrations lethal to 10%, 25%, and 50%, respectively, of cells (Figure 3, A and data not shown).

5AHQ Binding to the 20S Proteasome

Given that 5AHQ inhibits the proteasome through a unique mechanism, we evaluated its interaction with this complex by NMR. Our initial NMR studies to examine the interaction between 5AHQ and the full *T acidophilum* proteasome comprising α and β subunits were not successful because the elevated temperatures (65°C) and long recording times necessary to obtain high-quality NMR spectra of this 670 kDa complex (12–16 hours at a proteasome concentration of approximately 4 μM as was used here) (16) led to degradation of 5AHQ (data not shown). By contrast, NMR spectra of a smaller half-proteasome construct comprising a pair of heptameric α-rings (α_7-α_7; molecular mass = 360 kDa) can be recorded rapidly, and the spectra of the half-proteasome in complex with 5AHQ are of high quality, even at only 50°C. Therefore, we evaluated the interactions of 5AHQ with α_7-α_7.

The interaction of 5AHQ with α_7-α_7 produced clear spectral changes localized to residues Ile159, Val113, Val87, Val82, Leu112, Val89, Val134, Val24, and Leu136, all of which are

Table 1. IC_{50} values of 5-amino-8-hydroxyquinoline (5AHQ) in leukemia and myeloma cell lines*

	Mean IC_{50}, μM (95% CI)		
Cell line†	**Proteasome inhibition in cell extracts**	**Proteasome inhibition in intact cells**	**Cell viability**
Leukemia			
AML2	4.2 (3.61 to 4.79)	3.89 (3.78 to 4.00)	3.46 (3.13 to 3.79)
NB4	2.4 (2.22 to 2.58)	2.15 (1.82 to 2.48)	1.38 (1.34 to 1.42)
KG1A	5.3 (4.53 to 6.07)	5.03 (4.17 to 5.89)	3.85 (3.27 to 4.43)
MDAY-D2 (mouse)	2.64 (2.17 to 3.11)	0.57 (0.47 to 0.61)	1.96 (1.85 to 2.07)
Myeloma			
UTMC2	2.54 (2.34 to 2.74)	2.62 (2.44 to 2.80)	2.29 (2.17 to 2.41)
KMH11	1.32 (0.94 to 1.70)	3.96 (3.89 to 4.03)	0.94 (0.9 to 0.98)
KMS18	0.57 (0.56 to 0.58)	2.23 (1.98 to 2.48)	1.31 (1.21 to 1.41)

* To measure the effects of 5AHQ on the proteasomal activity in cell extracts, cellular proteins were extracted from leukemia and myeloma cell lines and treated with increasing concentrations of 5AHQ for 2 hours. To measure the effects of 5AHQ on the proteasomal activity in intact cells, leukemia and myeloma cell lines were treated with increasing concentrations of 5AHQ for 22 hours and then cellular proteins were extracted. The fluorogenic substrate Suc-LLVY-AMC (7-amino-4-methylcoumarin) was added to equal concentrations of proteins, and the rate of free AMC was measured over time. Data represent the mean values and 95% CIs relative to untreated control cells. Experiments were performed in duplicate and repeated twice (n = 4). To measure the effects of 5AHQ on cell viability, leukemia and myeloma cell lines were treated with increasing concentrations of 5AHQ for 72 hours. After treatment, cell viability was measured by the AlamarBlue fluorescence assay. Data represent the mean values and 95% CIs relative to cells treated with buffer alone. Experiments were performed at least in duplicate and repeated at least twice (n = 8–10). CI = confidence interval; IC_{50} = concentration that caused a 50% loss of proteasome activity or cell viability compared with untreated control cells.

† Human unless otherwise indicated.

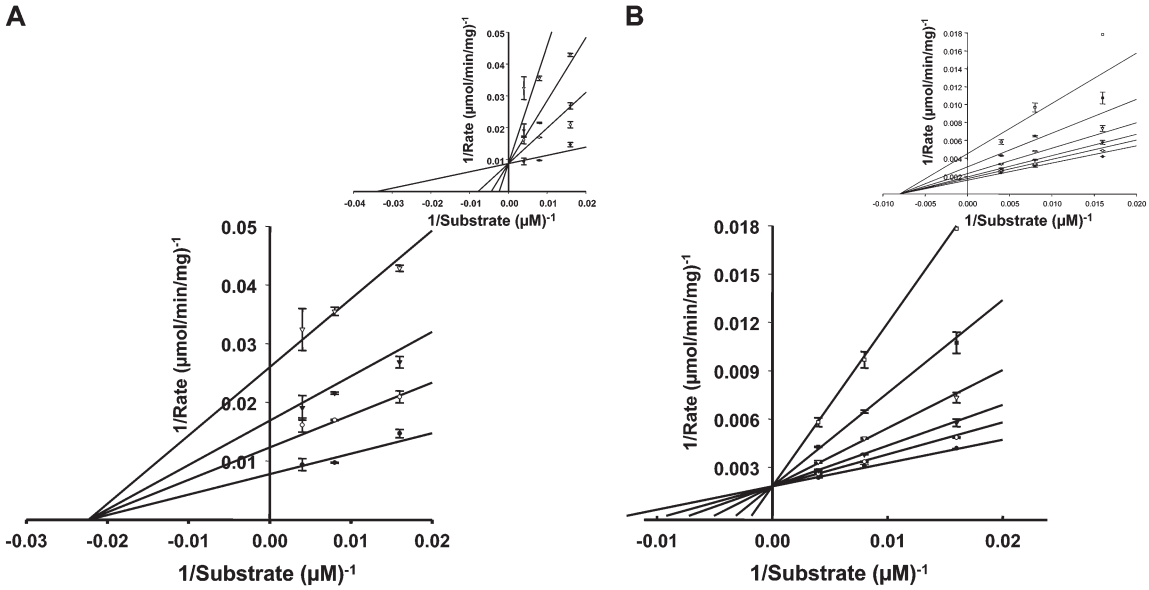

Figure 2. Effect of 5-amino-8-hydroxyquinoline (5AHQ) on isolated proteasomes. Proteasomes isolated from rabbit muscle were treated for 1 hour with 0 µM (**black circle**), 1.25 µM (**open circle**), 2.5 µM (**black triangle**), or 5 µM (**open triangle**) 5AHQ (**A**) or 0 µM (**black circle**), 0.078 µM (**open circle**), 0.156 µM (**black triangle**), 0.312 µM (**open triangle**), 0.625 µM (**black square**), or 1.25 µM (**open square**) MG132 (**B**). After incubation, the fluorogenic substrate Z-LLE-AMC (7-amino-4-methylcoumarin) was added at increasing concentrations (31.25, 62.5, 125, and 250 µM) and free AMC was measured over time with the use of a florescence spectrophotometric plate reader (excitation = 380 nm, emission = 460 nm). Data points represent the mean rate of AMC release from an experiment performed in triplicate (n = 3); error bars correspond to 95% confidence intervals. Lineweaver–Burk plots are presented as a fit to a noncompetitive model of inhibition for 5AHQ (**A**) and a competitive model for MG132 (**B**). Insets: Lineweaver–Burk plots are presented demonstrating a poor fit to a competitive model of inhibition for 5AHQ and a noncompetitive model for MG132.

located inside the regulatory antechamber of the proteasome and outside of the catalytic site in the proteolytic chamber (data not shown and Figure 3, B). By contrast, MG132, which binds the catalytic sites of the β subunits in the proteolytic chamber, produced shifts in the β rings of the full archaebacterial proteasome (data not shown) as expected and as previously described (13). Thus, 5AHQ interacts with the antechamber of the proteasome at a site distinct from the active site where other proteasome inhibitors such as MG132 and bortezomib bind. However, because these NMR studies were conducted using α_7-α_7, we cannot exclude the possibility that 5AHQ also interacts with sites on the β subunits.

Effect of 5AHQ on the Proteasome in Intact Cells

Given the ability of 5AHQ to inhibit the enzymatic activity of the proteasome in cell extracts, we next assessed the effects of 5AHQ on proteasome function in intact cells. OCI-AMl2, NB4, KG1A, and MDAY-D2 leukemia and UTMC2, KMH11, and KMS18 myeloma cell lines were treated with increasing concentrations of 5AHQ for 22 hours. The cells were harvested and lysed, and the chymotrypsin-like activity of the proteasome was measured by monitoring the rate of cleavage of the fluorescent substrate Suc-LLVY-AMC. 5AHQ inhibited the rate of Suc-LLVY-AMC cleavage in the malignant cell lines with mean IC_{50}s of less than 5 µM (mean IC_{50} for inhibition of the proteasome in intact cells, OCI-AML2: 3.89 µM, 95% CI = 3.78 to 4.00 µM; NB4: 2.15 µM, 95% CI = 1.82 to 2.48 µM; KG1A: 5.03 µM, 95% CI = 4.17 to 5.89 µM; MDAY-D2: 0.57 µM, 95% CI = 0.47 to 0.61 µM; UTMC2: 2.62 µM, 95% CI = 2.44 to 2.80 µM; KMH11: 3.96 µM, 95% CI = 3.89 to 4.03 µM; KMS18: 2.23 µM, 95% CI = 1.98 to 2.48 µM). Thus, 5AHQ inhibits the enzymatic activity of the proteasome in intact tumor cells (Table 1). Of note, 5AHQ did not alter levels of the proteasomal enzymes: We observed no change in expression of the β5 proteasome subunit when 5AHQ was added to intact cells at concentrations up to 10 µM for 24 hours (data not shown). Likewise, 5AHQ did not alter the β5 levels when added to cell extracts (data not shown).

To further assess the effects of 5AHQ on the function of the proteasome in intact cells, human myeloma LP1 cells were treated for 24 hours with increasing concentrations of 5AHQ. The cells were harvested, lysates of total protein were prepared, and equal amounts of protein were subjected to immunoblot analysis to examine the abundance of ubiquitinated proteins in the cells. At concentrations as low as 2.5 µM, 5AHQ increased the amount of ubiquitinated protein compared with the amount in untreated samples, consistent with inhibition of the proteasome (Figure 4, A).

Through its effects on the proteasome, bortezomib inhibits the NF-Kappa B signaling pathway, which is important for cellular proliferation (28). Therefore, we evaluated the effect on 5AHQ on NF-Kappa B signaling in cells. MDAY-D2 cells were treated with increasing concentrations of 5AHQ for 24 hours, followed by treatment for 1 hour with TNF-α to stimulate NF-Kappa B signaling or buffer control to evaluate basal NF-Kappa B signaling. The cells were harvested, nuclear protein extracts were prepared, and binding of the NF Kappa B p65 subunit to a consensus DNA-binding sequence (which is required for signaling) was measured by a chemiluminescent-based enzyme-linked immunosorbent assay as an indicator of NF Kappa B signaling. 5AHQ inhibited

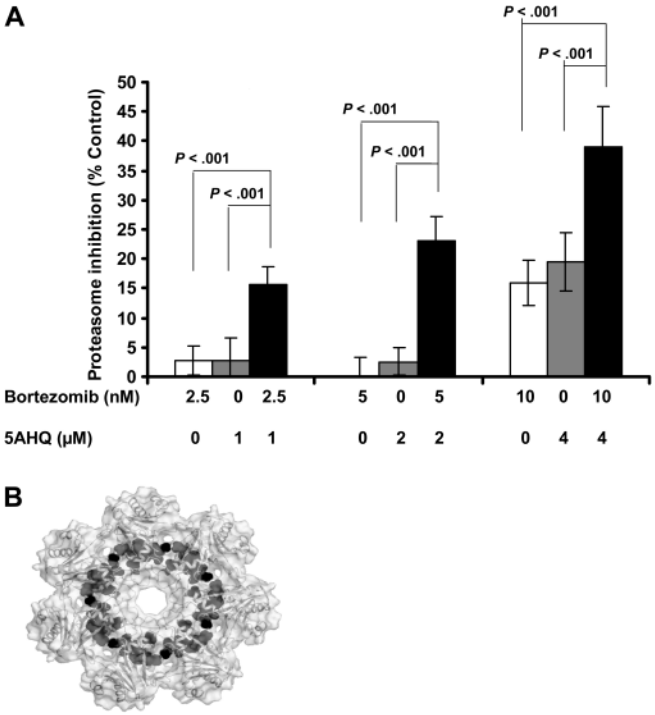

Figure 3. Effect of the combination of 5-amino-8-hydroxyquinoline (5AHQ) and bortezomib on proteasome activity. **A**) Proteasome inhibition assay. Proteasomes isolated from rabbit muscle were treated for 1 hour with the indicated concentrations of bortezomib (**gray bars**), 5AHQ (**white bars**), or the combination of bortezomib and 5AHQ (**black bars**). After incubation, the release of free 7-amino-4-methylcoumarin (AMC) from the fluorogenic substrate Z-LLE-AMC was measured using a florescence spectrophotometric plate reader (excitation = 380 nm, emission = 460 nm). Data represent mean proteasomal activity as defined by the amount of free AMC in treated cells divided by the amount of free AMC untreated control cells multiplied by 100. Experiments were performed at least in duplicate and repeated three times (n = 6); **error bars** represent 95% confidence intervals. All *P* values are from two-sided *t* tests. **B**) Molecular model. Inside view of the α-rings of the *Thermoplasma acidophilum* half-proteasome highlighting residues (**darkened region**) that are affected in nuclear magnetic resonance spectra upon addition of 5AHQ.

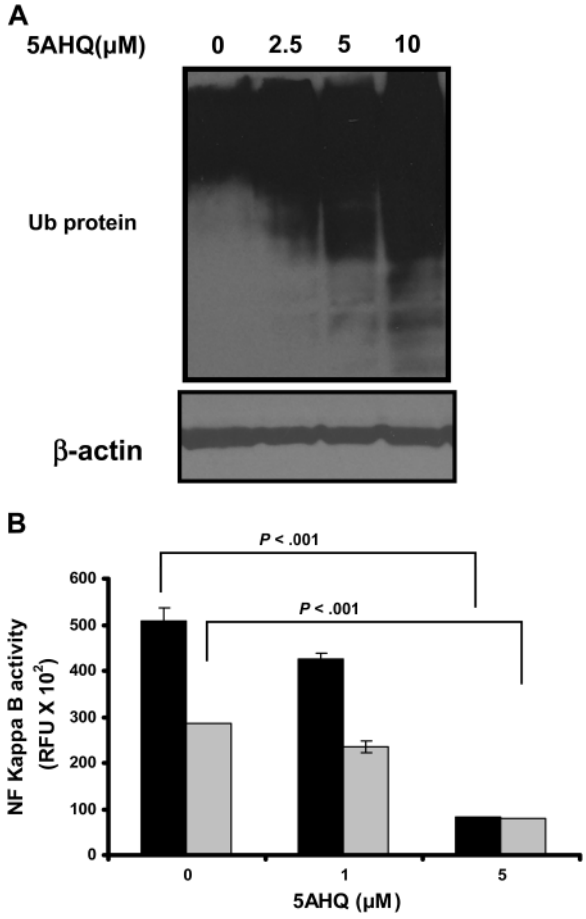

Figure 4. Effect of 5-amino-8-hydroxyquinoline (5AHQ) on proteasome activity when added to intact cells. **A**) Immunoblot analysis of ubiquitinated proteins. Multiple myeloma LP1 cells were treated with increasing concentrations of 5AHQ for 24 hours, then harvested, total protein was isolated, and equal concentrations of protein were subjected to immunoblot analysis with anti-ubiquitin and anti-β-actin antibodies to assess the abundance of ubiquitinated proteins and β-actin expression, respectively. **B**) NF-Kappa B activity. Mouse leukemia MDAY-D2 cells were treated with increasing concentrations of 5AHQ for 24 hours followed by treatment for 1 hour with 10 nM tumor necrosis factor alpha (**black bars**) or buffer control (**gray bars**). The cells were harvested, nuclear proteins were extracted, and NF-Kappa B activity was measured based on the ability of the p65 subunit to bind its DNA consensus sequence using an enzyme-linked immunosorbent assay as described in the "Materials and Methods." Data represent the mean values of NF-Kappa B activity in relative chemiluminescent units (RLU) from three experiments performed in triplicate (n = 9); **error bars** correspond to 95% confidence intervals. *P* values are from two-sided *t* tests.

both basal and TNF-α–stimulated NF-Kappa B activity at concentrations at which it inhibited the enzymatic activity of the proteasome (mean basal NF-Kappa B activity: 0 vs 5 μM 5AHQ = 28 682.3 vs 7944.8 relative chemiluminescent units [RLU], difference = 20 737.5 RLU, 95% CI = 20 661.4 to 20 813.8 RLU, $P < .0001$; mean TNF-α–stimulated NF-Kappa B activity: 0 vs 5 μM 5AHQ = 50 946.5 vs 8176.2 RLU, difference = 42 770.3 RLU, 95% CI = 40 171.1 to 45 369.4 RLU; $P < .001$) (Figure 4, B).

Induction of Cell Death by 5AHQ in Malignant Cells and Normal Cells

Inhibition of the proteasome induces cell death in malignant cells (4). Therefore, we assessed the effects of 5AHQ on cell viability in malignant cell lines and in primary malignant cells isolated from patients with leukemia and myeloma. Human (OCI-AML2, NB4, and KG1A) and mouse (MDAY-D2) leukemia cells and human myeloma UTCMC2, KMH111, and KMS18 cells were treated with increasing concentrations of 5AHQ for 72 hours, and cell viability was measured by the AlamarBlue assay. Concentrations of 5AHQ required to inhibit 50% inhibition of growth (IC_{50}s) were in the low micromolar range (mean IC_{50} for inhibition of cell growth, OCI-AML2: 3.46 μM, 95% CI = 3.13 to 3.79 μM; NB4: 1.38 μM, 95% CI = 1.34 to 1.42 μM; KG1A: 3.85 μM, 95% CI = 3.27 to 4.43 μM; MDAY-D2: 1.96 μM, 95% CI = 1.85 to 2.07 μM; UTMC2: 2.29 μM, 95% CI = 2.17 to 2.41 μM; KMH11: 0.94 μM, 95% CI = 0.9 to 0.98 μM; KMS18: 1.31 μM, 95% CI = 1.21 to 1.41 μM) (Table 1). Cell death was confirmed by annexin V staining (data not shown).

We also tested the effects of 5AHQ on the viability of primary malignant and normal hematopoietic cells isolated from patient samples. Primary AML, CLL, multiple myeloma, and normal PBSC were treated with increasing concentrations of 5AHQ for 48 hours. After incubation, cell viability was measured by MTS

(AML and normal PBSC), AlamarBlue (CLL), and annexin V staining (myeloma). 5AHQ induced cell death in primary AML, CLL, and myeloma cells with IC_{50}s in the low micromolar range (Figure 5, A and B). By contrast, 5AHQ was not cytotoxic to normal PBSC at concentrations up to 62.5 μM (62.5 μM 5AHQ: mean relative percentage of viable PBSC vs AML cells = 85.1% vs 30.6%, difference = 54.5%, 95% CI = 31.8% to 76.9%, $P < .001$; 62.5 μM 5AHQ: mean relative percentage of viable PBSC vs CLL cells = 85.1% vs 13.2%, difference = 71.9%, 95% CI = 52.4% to 91.3%, $P < .001$; 31.25 μM 5AHQ: mean relative percentage of viable PBSC vs AML cells = 92.5% vs 30%, difference = 62.5%, 95% CI = 32.7% to 92.3%, $P < .001$; 31.25 μM 5AHQ: mean relative percentage of viable PBSC vs CLL cells = 92.5% vs 10.5%, difference = 82%, 95% CI = 57% to 107%, $P < .001$) (Figure 5, A and B).

Combined Effect of 5AHQ and Bortezomib on Cell Viability

The combination of 5AHQ and bortezomib synergistically inhibited the proteasome (Figure 3, A). We therefore evaluated the cytotoxicity of these two inhibitors in OCI-AML2 cells treated for 48 hours with increasing concentrations of the two compounds. 5AHQ acted synergistically with bortezomib to induce cell death at levels greater than those observed with either compound alone, with CIN values of 0.31, 0.48, and 0.74 at the concentration of 5AHQ and bortezomib lethal to 10%, 25%, and 50%, respectively, of cells (Figure 5, C and data not shown).

Effect of 5AHQ on Cell Viability in Bortezomib-Resistant Cells

The efficacy of bortezomib as an anticancer drug for patients with hematologic malignancies is hampered by the emergence of drug resistance, which may be due, in part, to overexpression and mutation of the β5 proteasome subunit to which bortezomib binds (11) or to overexpression of multidrug-resistant pump proteins (29). Given that 5AHQ inhibited the proteasome through a mechanism distinct from that of bortezomib, we evaluated the cytotoxictiy of 5AHQ in human leukemia THP1 cells that were selected for their resistance to increasing concentrations of bortezomib and that overexpress a mutated β5 proteasome subunit (11). We treated THP1/BTZ50, THP1/BTZ100, THP1/BTZ100, and THP1/BTZ500 cells with increasing concentrations of 5AHQ (in the absence of bortezomib) or bortezomib for 72 hours and then measured cell viability by use of a trypan blue assay. THP1/BTZ50, THP1/BTZ100, THP1/BTZ100, and THP1/BTZ500 cells, which are 45-, 79-, 129-, and 237-fold more resistant to bortezomib, respectively, compared with wild-type THP1 cells, had essentially the same sensitivity to 5AHQ-induced cell death as THP1 cells (10) (mean IC_{50} for 5AHQ in the absence of bortezomib: THP1/WT: 3.7 μM [95% CI = 3.4 to 4.0 μM]; THP1/BTZ50: 6.6 μM [95% CI = 6.2 to 7.0 μM]; THP1/BTZ100: 6.3 μM [95% CI = 5.9 to 6.7 μM]; THP1/BTZ200: 6.4 μM [95% CI = 5.7 to 7.1 μM]; THP1/BTZ500: 6.6 μM [95% CI = 5.9 to 7.5 μM]). Similar results were obtained when the cells were treated with 5AHQ in presence of bortezomib (Table 2).

To further test the ability of 5AHQ to induce cell death in cells resistant to bortezomib, we examined the effect of 5AHQ cell viability and proteasome activity in K562 cells, which are naturally resistant to bortezomib. Compared with MY5 myeloma and OCI-AML2 leukemia cells, K562 leukemia cells overexpress the β5 proteasome subunit (Figure 6, A). Compared with MY5 and OCI-AML2 cells, K562 cells were more resistant to bortezomib-mediated inhibition of proteasomal enzymatic activity (Figure 6, B)

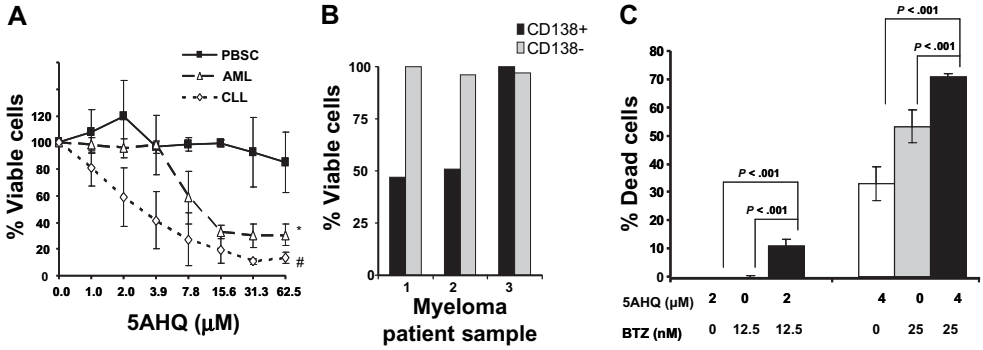

Figure 5. Cytotoxicity of 5-amino-8-hydroxyquinoline (5AHQ), alone and in combination with bortezomib, in malignant cells vs normal hematopoietic cells. **A**) Growth and viability of primary cells treated with 5AHQ. Primary acute myeloid leukemia (AML) blasts (**open triangles**) (n = 4), chronic lymphocytic leukemia (CLL) (**open diamonds**) (n = 5), or normal peripheral blood stem cells (PBSCs) (**black squares**) (n = 4) were obtained from the peripheral blood of consenting patients with AML and CLL or donors of PBSC for allotransplantation, respectively. Mononuclear cells were isolated by Ficoll separation and treated for 48 hours with increasing concentrations of 5AHQ. Cell viability was measured by the (3-(4,5-dimethylthiazol-2-yl)-5-(3-carboxymethoxyphenyl)-2-(4-sulfophenyl)-2*H*-tetrazolium inner salt) MTS (AML and PBSC) or AlamarBlue fluorescence (CLL) assay. Data represent the mean percentage of viable cells in treated vs untreated controls tested in triplicate (n = 12–15). **Error bars** correspond to 95% confidence intervals. #$P < .001$ for PBSC vs AML at 62.5 μM 5AHQ (two-sided *t* test); *$P < .001$ for PBSC vs CLL at 62.5 μM 5AHQ (two-sided *t* test). **B**) Viability of primary myeloma cells treated with 5AHQ. Bone marrow samples were obtained from three patients with multiple myeloma. Mononuclear cells were isolated by Ficoll separation and treated for 48 hours with 5 μM 5AHQ or buffer control. Viability of the myeloma (CD138 positive, **black bars**) and normal hematopoietic (CD138 negative, **gray bars**) cells was measured by costaining with phycoerythrin-labeled anti-CD138 and fluorescein isothiocyanate–labeled annexin V and flow cytometry. Data represent the percentages of viable cells in three individual patient samples. **C**) Cell death with the combination of 5AHQ and bortezomib (BTZ). OCI-AML2 cells were treated for 48 hours with the indicated concentrations of 5AHQ (**white bars**), bortezomib (**gray bars**), or both agents combined (**black bars**). Cell viability was measured by annexin V and propidium iodide staining. Data represent mean percentage of dead cells in treated sample relative to untreated control cells. Experiments were performed in duplicate and repeated twice (n = 4); **error bars** correspond to 95% confidence intervals. *P* values are from two-sided *t* tests.

Table 2. Growth inhibitory effects of 5-amino-8-hydroxyquinoline (5AHQ) against human leukemia cells with acquired resistance to bortezomib*

Cell line	Mean IC_{50}, μM (95% CI)	Resistance factor†	
		5AHQ	Bortezomib‡
THP1/WT	3.7 (3.4 to 4.0)	1	1
THP1/BTZ50			
−bortezomib	6.6 (6.2 to 7.0)	1.8	45
+bortezomib	5.9 (5.5 to 6.3)	1.6	
THP1/BTZ100			
−bortezomib	6.3 (5.9 to 6.7)	1.7	79
+bortezomib	6.2 (5.2 to 5.8)	1.7	
THP1/BTZ200			
−bortezomib	6.4 (5.7 to 7.1)	1.7	129
+bortezomib	6.2 (5.8 to 6.6)	1.7	
THP1/BTZ500			
−bortezomib	6.6 (5.9 to 7.5)	1.8	237
+bortezomib	5.3 (5.5 to 6.1)	1.4	

* Human leukemia THP1/BTZ50, THP1/BTZ100, THP1/BTZ200, and THP1/BTZ500 cells were grown in the absence or presence of 50, 100, 200, or 500 nM bortezomib, respectively, for at least 3 days and then were treated with increasing concentrations of 5AHQ or bortezomib for 72 hours. After incubation, cell viability was assessed by trypan blue staining. Data represent the mean values and 95% CIs for three separate experiments performed in triplicate (n = 9). CI = confidence interval; IC_{50} = concentration that caused a 50% loss of cell viability compared with untreated control cells.

† IC_{50} resistant cell line/IC_{50} parental cell line (THP1/WT).

‡ Data from Oerlemans et al. 2008 (11).

and bortezomib-induced cell death (Figure 6, C). However, K562 cells remained fully sensitive to proteasome inhibition and cell death by 5AHQ, consistent with a mechanism of proteasome inhibition distinct from bortezomib (Figure 6). We also examined the effect of 5AHQ on cell viability in leukemia CEM cells, which are resistant to a variety of chemotherapeutic drugs (30–33) including bortezomib due to overexpression of the multidrug-resistant pumps P glycoprotein, breast cancer resistance protein, or multidrug resistance protein 1. These multidrug-resistant cells also remained equally sensitive to 5AHQ-induced cell death compared with CEM wild-type cells (data not shown). Thus, 5AHQ can overcome at least some forms of bortezomib resistance and does not appear to be a substrate for common multidrug resistance drug efflux transporters that can confer a multidrug-resistant phenotype.

Effect of 5AHQ on Tumor Growth in Xenograft Models

We next evaluated the effects of oral administration of 5AHQ on tumor growth in three mouse models of leukemia. Sublethally irradiated NOD/SCID mice were injected subcutaneously with human leukemia OCI-AML2 or K562 cells or intraperitoneally with murine leukemia MDAY-D2 cells. The day after injecting the MDAY-D2 cells or approximately 1 week after K562 and OCI-AML2 cell injection, when the subcutaneous tumors were palpable, the mice were treated once per day for 8 days (MDAY-D2) or 10 days (K562 and OCI-AML2) with 5AHQ (50 mg/kg body weight) or buffer control by oral gavage (MDAY-D2 and K562: n = 10 mice per group; OCI-AML2: n = 9 mice per group). The mice were monitored daily for changes in behavior and body weight, and at the end of the treatment period, the tumors were excised and weighed. In all three mouse models, compared with control, orally administered 5AHQ suppressed tumor growth without causing weight loss or signs of organ toxicity (OCI-AML2 model: median tumor weight [interquartile range {IQR}], 5AHQ vs control = 95.7 mg [61.4–163.5 mg] vs 247.2 mg [189.4–296.2 mg],

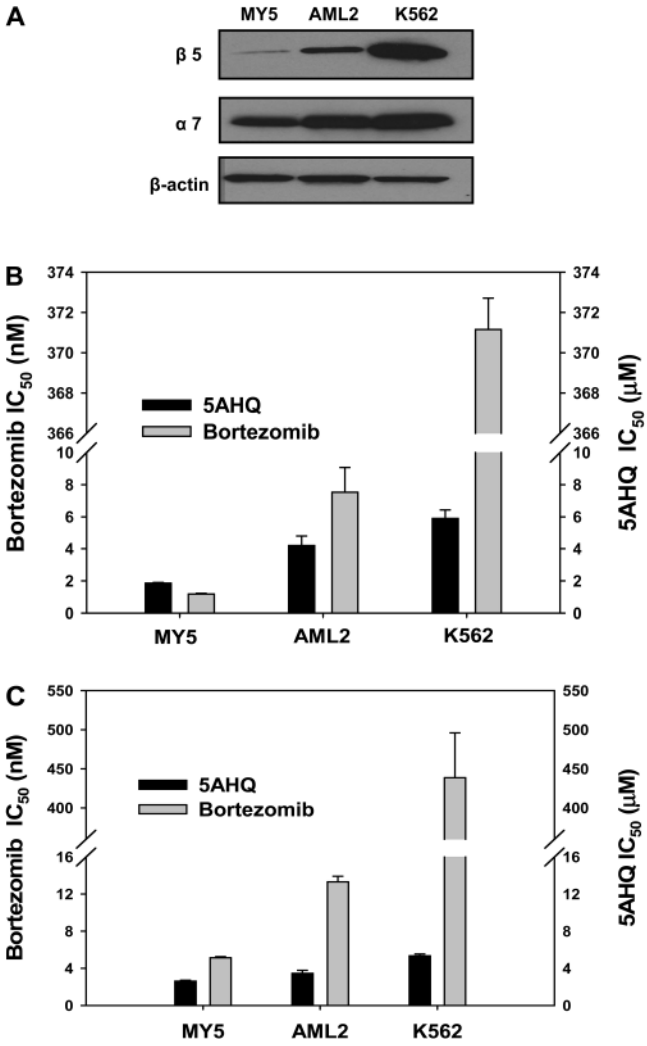

Figure 6. Cytotoxicity of 5-amino-8-hydroxyquinoline (5AHQ) in bortezomib-resistant cell lines. **A**) Immunoblot analysis of β5 and α7 subunit expression. The abundance of the β5 subunit and α7 subunit of the proteasome and β-actin expression was assessed by immunoblotting with anti-β5 subunit, anti-α7 subunit and anti-β-actin antibodies, respectively, in protein lysates from My5, OCI-AM2, and K562 cells. **B**) Proteasome inhibition. Cellular proteins were extracted from My5, OCI-AM2, and K562 cells and treated with increasing concentrations of 5AHQ (**black bars**) or bortezomib (**gray bars**) for 2 hours. After incubation, the fluorogenic substrate Suc-LLVY-AMC (7-amino-4-methylcoumarin) was added and the rate of free AMC was measured over time as described in "Materials and Methods." Data represent the mean IC_{50}s, where IC_{50} represents the concentration of drug required to inhibit 50% of the proteasomal activity of buffer-treated cells. Experiments were performed in duplicate and repeated twice (n = 4); **error bars** correspond to 95% confidence intervals. **C**) Cell growth. My5, OCI-AM2, and K562 were treated for 72 hours with increasing concentrations of 5AHQ (**black bars**) or bortezomib (**gray bars**). After treatment, cell viability was measured by the AlamarBlue fluorescence assay. Data represent mean IC_{50}s (**error bars** correspond to 95% confidence intervals), where the IC_{50} represents the concentration of drug required to reduce cellular growth by 50% of buffer-treated cells. Experiments were performed in duplicate and repeated two to 10 times (n = 4–20).

P = .002; K562 model: median tumor weight [IQR], 5AHQ vs control = 105 mg [40.8–178.4 mg] vs 209.5 mg [134.9–267 mg], P = .01; MDAY-D2 model: median tumor weight [IQR], 5AHQ vs control = 819.9 mg [551.7–1111.5 mg] vs 1163.1 mg [1024.9–1281.3 mg], P = .001) (Figure 7, A–C).

We examined the effects of 5AHQ on proteasome activity in the OCI-AML2 xenograft model by adding the fluorogenic proteasome substrate Suc-LLVY-AMC to protein lysates made from the excised OCI-AML2 tumor xenografts and measuring the generation of free AMC. Proteasome activity (expressed as relative fluorescence units [RFU] of free AMC) was lower in tumor lysates from mice treated with 5AHQ than in tumor lysates from mice treated with buffer control (mean proteasome activity, 5AHQ vs control: 1221.16 vs 1921.58 RFU, difference = 700.42 RFU, 95% CI = 191.08 to 1209.76 RFU; P = .008 [t test]) (Figure 7, D).

To partially characterize the pharmacokinetics of 5AHQ, NOD/SCID mice bearing subcutaneous MDAY-D2 tumors were treated 1 week after tumor cell injection with a single dose of 5AHQ (50 mg/kg body weight) by oral gavage. At increasing times after treatment, mice (n = 3 per time point) were killed by CO_2 inhalation and their plasma and tumors were collected and subjected to mass spectrometry to measure levels of 5AHQ and conversion products and metabolites of 5AHQ. 5AHQ was detected in the plasma at 15 minutes after dosing with a median peak concentration (C_{max}) of 2.3 μg/mL (IQR = 1.4–6.75 μg/mL) (equivalent to 14.3 μM). Also detected in the plasma at 15 minutes after dosing were the oxidized form of 5AHQ (dihydroxyquinoline) with a median C_{max} of 0.23 μg/mL (IQR = 0.14–0.39 μg/mL) (equivalent to 1.4 μM) and glucuronidated 5AHQ with a median C_{max} of 18.6 μg/mL (IQR = 13.2–32.0 μg/mL) (equivalent to 115 μM). At 30 minutes after dosing, 5AHQ was detected in the tumors with a median C_{max} of 0.39 μg/mL (IQR = 0.27–1.78 μg/mL) (equivalent to 2.4 μM). Also detected in the tumors at 30 minutes after dosing were dihydroxyquinoline, with a median C_{max} of 0.03 μg/mL (IQR = 0.0–0.04 μg/mL) (equivalent to 0.18 μM), and glucuronidated 5AHQ, with a median C_{max} of 0.54 μg/mL (IQR = 0.29–1.5 μg/mL) (equivalent to 3.3 μM).

To better understand the potential toxicity of 5AHQ, mice (n = 5 of each sex) were treated with 5AHQ at 0 (control), 100, 200, or 300 mg/kg body weight/d by oral gavage daily for 14 days. An additional five mice of each sex were assigned to the control and highest dose groups for a 1-week recovery during which mice received no 5AHQ for 7 days after the 14-day treatment period. In the highest dose group, the dose of 5AHQ was increased to 450/kg body weight/d starting on day 10 because no overt toxic effects were observed. At the completion of the treatment and recovery periods, mice were killed, their blood sent for chemistry and hematology analysis, and their organs were observed for gross signs of toxic effects. The only detectable toxic effect was an increase in the plasma level of aspartate aminotransferase (AST), a marker of liver inflammation, in male mice that were treated with the highest dose of 5AHQ compared with control (Table 3), which was reversed during the 1-week recovery period (mean AST level on day 14 of treatment, 0 vs 300 (increased to 450 on day 10) mg/kg/d 5AHQ = 39.6 vs 140.4 U/L, difference = 100.8 U/L, 95% CI = 188.6 to 13.04 U/L, P < .001; mean AST level after 1-week recovery, 0 vs 300 (increased to 450 on day 10) mg/kg/d 5AHQ: 35.2 vs 39.1 U/L, difference = 3.9 U/L, 95% CI = −3.1 to 10.5 U/L, P = .79). We also detected a non-statistically significant increase in total bilirubin in male mice treated for 14 days with 300 mg/kg/d (increased to 450 mg/kg/d on day 10) 5AHQ compared with control that was also reversed during the 1-week recovery period

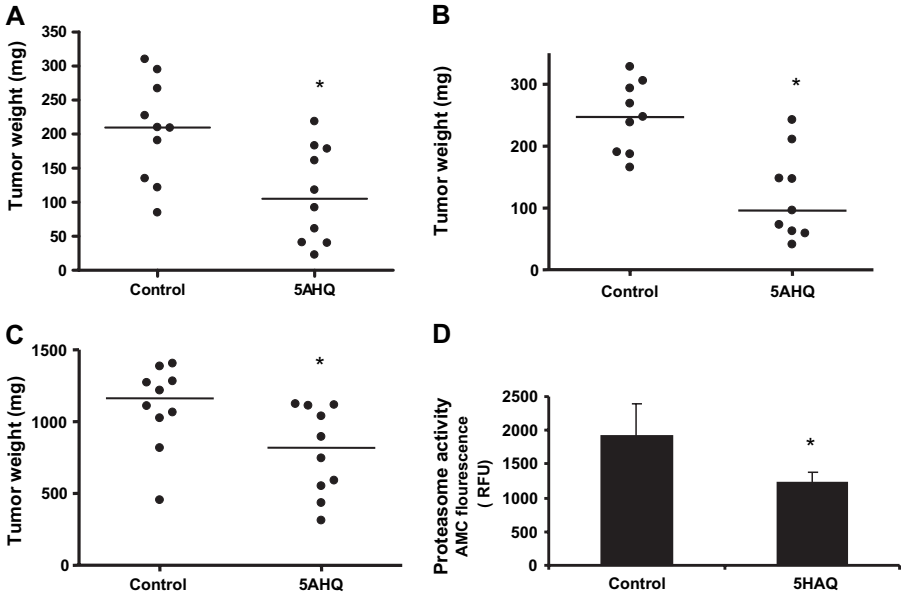

Figure 7. Effect of 5-amino-8-hydroxyquinoline (5AHQ) on tumor growth in mouse models of leukemia. (**A–C**) Scatter plot analyses of final tumor weights. Sublethally irradiated nonobese diabetic/severe combined immunodeficient (NOD/SCID) mice were injected subcutaneously with K562 (**A**) or OCI-AML2 (**B**) leukemia cells or intraperitoneally with MDAY-D2 (**C**) leukemia cells. Starting the day after tumor injection (MDAY-D2) or approximately 7 days after injection when the tumors were palpable (K562 and OCI-AML2), mice were treated daily for 8 (MDAY-D2) or 10 (OCI-AML2 and K562) days by oral gavage with buffer or 50 mg 5AHQ/kg body weight dissolved in buffer (0.4% Tween 80 in phosphate-buffered saline) (n = 10 mice per treatment group for K562 and MDAY-D2 and n = 9 per treatment group mice for OCI-AML2). The mice were killed, the subcutaneous or intraperitoneal tumors were excised, and the weights of the tumors were measured. **Horizontal bars** indicate the median values. **Asterisks** indicate statistically significant differences for 5AHQ vs control (K562: P = .01; OCI-AML2: P = .002; MDAY-D2: P = .001) by the Mann–Whitney nonparametric test (two-sided). **D**) Proteasome activity in OCI-AMI2 xenograft tumors. OCI-AML2 leukemia xenograft tumors were excised from the mice treated with 5AHQ (n = 9) or buffer control (n = 9) (described above), and protein extracts were made. To equal concentrations of protein, the proteasome fluorogenic substrate, Suc-LLVY-AMC (7-amino-4-methylcoumarin), was added and the generation of free AMC was measured over time with a fluorescence spectrophotometric plate reader. Data represent mean free AMC fluorescence in relative fluorescence units (RFU), and **error bars** correspond to 95% confidence intervals (n = 9 tumors per treatment group) from the one experiment. **Asterisk** indicates statistically significant difference for control vs 5AHQ (P = .008, two-sided t test).

Table 3. Toxicology of 5-amino-8-hydroxyquinoline (5AHQ) in male mice*

Treatment group	ALT, U/L	AST, U/L	ALP, U/L	TBil, μmol/L	BUN, mmol/L	Cr (μmol/L)
Control	23.2 (18.5 to 27.9)	39.6 (31.8 to 47.4)	139.3 (103.3 to 175.3)	2.0 (0.84 to 3.09)	7.8 (5.85 to 9.67)	9.8 (7.68 to 11.9)
5AHQ	36.6 (19.9 to 53.3)	140.4 (35.0 to 245.8)	79.3 (44.6 to 114)	3.3 (1.7 to 5.0)	5.3 (2.3 to 8.4)	6.3 (3.4 to 9.2)
Difference†	13.4 (−1.0 to 27.8)	100.8 (13.0 to 188.6)	−60 (−101.6 to −18.49)	1.3 (−0.3 to 3.0)	−2.4 (−5.4 to 0.6)	1.5 (−4.3 to 1.4)
P‡	.06	<.001	.01	.09	.10	.2
Control recovery	25.7 (21.9 to 29.45)	35.25 (27.4 to 43.1)	147.1 (107.5 to 186.7)	2.4 (2.1 to 2.8)	8.0 (7.2 to 8.7)	7.8 (7.2 to 8.5)
5AHQ recovery	23.4 (14.6 to 32.3)	39.1 (30.0 to 48.3)	150.0 (117 to 182.6)	0.7 (0.1 to 1.3)	9.6 (7.0 to 12.1)	11.7 (5.5 to 17.9)
Difference§	1.9 (−7.3 to 3.5)	3.7 (−3.1 to 10.5)	7.5 (−23.2 to 38.2)	−1.8 (−2.3 to −1.4)	1.9 (0.2 to 3.5)	4.1 (0.5 to 7.6)
P‡	.48	.79	.87	<.001	.03	.03

* CD1 male mice (n = 5 mice per group) were treated with 5AHQ at 300 mg/kg body weight/d or buffer control by oral gavage daily for 14 days. An additional five mice were assigned to the control group and to the highest dose group for a 1-week recovery period during which the mice received no drug for 1 week after the 14-day treatment. In the high-dose group, the dose of 5AHQ was increased to 450 mg/kg body weight/d starting on day 10 because no overt toxic effects were observed. At the completion of the experiment, mice were killed and their blood was sent for chemistry analysis. Data represent mean values and 95% confidence intervals. ALT = alanine transaminase; ALP = alkaline phosphatase; AST = aspartate aminotransferase; BUN = blood urea nitrogen; Cr = creatinine; TBil = total bilirubin.

† 5AHQ vs control.

‡ 5AHQ recovery vs control recovery.

§ Two-sided *t* test.

(mean total bilirubin level on day 14, 0 vs 300 mg/kg/d 5AHQ = 2.0 vs 3.3 mmol/L, difference = 1.3 mmol/L, 95% CI = −0.3 to 3.01 mmol/L, $P = 0.09$). No changes in AST or bilirubin were observed in the female mice (data not shown). No differences in body weight, food consumption, hematology, or renal function were observed between mice that received buffer control and mice in any of the 5AHQ treatment groups. The only abnormality noted on necropsy was dark yellow discoloration of the liver in one male mouse that was treated with the highest dose of 5AHQ. Thus, 5AHQ was well tolerated in mice at doses up to sixfold higher than the dose required for antitumor effects.

Discussion

In this study, we identified 5AHQ, a quinoline-based compound, and showed that it inhibited the proteasome noncompetitively. Consistent with a mechanism of action distinct from bortezomib, 5AHQ was cytotoxic to cells that are resistant to bortezomib. Finally, 5AHQ induced cell death in primary myeloma and AML cells preferentially over normal hematopoietic cells. Moreover, it inhibited tumor growth in mouse models of leukemia.

Proteasome inhibitors improve the clinical outcome of patients with multiple myeloma and mantle cell lymphoma and are currently being evaluated for the treatment of other malignancies, including leukemia (8,9,34). However, bortezomib and all of the other chemical proteasome inhibitors currently under clinical evaluation block the proteasome complex competitively by binding the active sites of the enzymes (5–7). Here, we describe the activity of 5AHQ, a proteasome inhibitor that is unique in that it inhibits the enzyme complex in a noncompetitive fashion. NMR studies established that 5AHQ binds the α subunits of the antechamber of the 20S proteasome, a novel binding site that is distinct from the binding site of bortezomib.

5AHQ induced cell death in leukemia and myeloma cell lines at the same concentrations at which it inhibited the proteasome and blocked NF-Kappa B signaling. These results suggest that the cytotoxicity of 5AHQ is related to its effects on the proteasome. Because 5AHQ and bortezomib inhibited the proteasome through distinct mechanisms, we evaluated the effect of these agents in combination in tumor cells. The combination of 5AHQ and bortezomib inhibited the proteasome and induced cell death in a synergistic fashion. Thus, combining competitive and noncompetitive proteasome inhibitors could be a novel strategy to increase response rates to proteasome inhibition in patients with leukemia or myeloma. Alternatively, if the side effect profiles of these two agents in patients are distinct, using them in combination could permit the use of lower doses of bortezomib, which would reduce the incidence and severity of bortezomib's toxic effects. Although our toxicology studies suggest that 5AHQ was well tolerated in mice, further investigation of the toxicology of 5AHQ in additional species is necessary before advancing this compound into clinical trials. In addition, toxicology studies with the combination of 5AHQ and bortezomib would be useful to determine whether the combination produces excessive or unexpected toxic effects.

Several mechanisms of bortezomib resistance have been identified, including increased levels of heat-shock protein 27 (35) and increased expression of multidrug resistance pumps (29). Previously, Oerlemans et al. (11) demonstrated that an acquired mutation in, or overexpression of, the β5 subunit of the proteasome can also confer resistance to bortezomib. Our finding that 5AHQ retained full activity in cell lines that carried mutated β5 subunits or that overexpressed β5 subunits is consistent with 5AHQ binding a site on the proteasome distinct from that of bortezomib. Moreover, 5AHQ retained activity in cells that overexpressed multidrug-resistant pumps. Therefore, 5AHQ overcomes some forms of bortezomib resistance. These findings support the development of 5AHQ or an analogue for the treatment of some patients with myeloma who relapse after bortezomib treatment. However, it is unknown how frequently mutations or overexpression of the β5 subunit occur in patients with bortezomib-resistant disease.

To our knowledge, the mechanism by which 5AHQ noncompetitively inhibits the proteasome is not known. However, one possibility is that 5AHQ binding outside of the active site produces a conformational change that prevents substrates from entering the proteolytic chamber of the proteasome complex. In 2003, Gaczynska et al. (36) showed that a 39-amino acid peptide named

PR39 binds the 20S proteasome and inhibits the enzyme noncompetitively. This peptide was postulated to bind to a site distal from the catalytic region and function via an allosteric mechanism of action whereby binding leads to changes in proteasome structure. However, characterization of the binding sites of PR39 on the proteasome has not yet, to our knowledge, been reported. More recently, we demonstrated that chloroquine also inhibits the proteasome noncompetitively by binding a region of the α subunits in the *T acidophilum* proteasome that is similar but does not overlap with the one that 5AHQ binds (13). However, chloroquine is a much weaker proteasome inhibitor than 5AHQ, and the concentrations of chloroquine that are required to inhibit the proteasome in intact mammalian cells are not pharmacologically achievable in animals or humans. Detailed crystal structures of the 5AHQ–proteasome interaction are needed to better discern the mechanism by which 5AHQ inhibits the proteasome. Furthermore, having a defined interaction site may lead to the development of more potent proteasome inhibitors, some of which could be leads for new therapeutic agents.

We recognized a number of limitations of this study. First, the experimental limitations discussed above prevented us from excluding the possibility that 5AHQ simultaneously binds to α and β subunits. However, the kinetic assays support a mechanism of inhibition that differs from that of bortezomib. Second, although results of the NMR studies suggest that 5AHQ has a direct effect on proteasomal function, we cannot exclude the possibility that a 5AHQ metabolite is primarily responsible for proteasome inhibition. In addition, we cannot fully exclude the possibility that 5AHQ or a metabolite also inhibits the proteasome through indirect effects. Finally, we cannot exclude the possibility that 5AHQ has additional targets beyond the proteasome and that inhibition of these other targets may also contribute to its anticancer effects.

In summary, we have found that 5AHQ is a novel noncompetitive inhibitor of the proteasome that synergizes with and overcomes resistance to the competitive proteasome inhibitor bortezomib. As such, 5AHQ may represent a new strategy for inhibition of the proteasome and a potential lead for a new class of therapeutic agents.

Supplementary Data

Supplementary data can be found at http://www.jnci.oxfordjournals.org/.

References

1. Goldberg AL. Protein degradation and protection against misfolded or damaged proteins. *Nature.* 2003;426(6968):895–899.
2. Nalepa G, Rolfe M, Harper JW. Drug discovery in the ubiquitin-proteasome system. *Nat Rev Drug Discov.* 2006;5(7):596–613.
3. Passmore LA, Barford D. Getting into position: the catalytic mechanisms of protein ubiquitylation. *Biochem J.* 2004;379(pt 3):513–525.
4. Hideshima T, Richardson P, Chauhan D, et al. The proteasome inhibitor PS-341 inhibits growth, induces apoptosis, and overcomes drug resistance in human multiple myeloma cells. *Cancer Res.* 2001;61(7):3071–3076.
5. Williamson MJ, Blank JL, Bruzzese FJ, et al. Comparison of biochemical and biological effects of ML858 (salinosporamide A) and bortezomib. *Mol Cancer Ther.* 2006;5(12):3052–3061.
6. Groll M, Huber R, Potts BC. Crystal structures of Salinosporamide A (NPI-0052) and B (NPI-0047) in complex with the 20S proteasome reveal important consequences of beta-lactone ring opening and a mechanism for irreversible binding. *J Am Chem Soc.* 2006;128(15):5136–5141.
7. Groll M, Berkers CR, Ploegh HL, et al. Crystal structure of the boronic acid-based proteasome inhibitor bortezomib in complex with the yeast 20S proteasome. *Structure.* 2006;14(3):451–456.
8. Richardson PG, Sonneveld P, Schuster MW, et al. Bortezomib or high-dose dexamethasone for relapsed multiple myeloma. *N Engl J Med.* 2005;352(24):2487–2498.
9. Fisher RI, Bernstein SH, Kahl BS, et al. Multicenter phase II study of bortezomib in patients with relapsed or refractory mantle cell lymphoma. *J Clin Oncol.* 2006;24(30):4867–4874.
10. McConkey DJ, Zhu K. Mechanisms of proteasome inhibitor action and resistance in cancer. *Drug Resist Updat.* 2008;11(4–5):164–179.
11. Oerlemans R, Franke NE, Assaraf YG, et al. Molecular basis of bortezomib resistance: proteasome subunit beta5 (PSMB5) gene mutation and overexpression of PSMB5 protein. *Blood.* 2008;112(6):2489–2499.
12. Mao X, Li X, Sprangers R, et al. Clioquinol inhibits the proteasome and displays preclinical activity in leukemia and myeloma. *Leukemia.* 2008;23(2):585–590.
13. Sprangers R, Li X, Mao X, et al. TROSY-based NMR evidence for a novel class of 20S proteasome inhibitors. *Biochemistry.* 2008;47(26):6727–6734.
14. Mao X, Stewart AK, Hurren R, et al. A chemical biology screen identifies glucocorticoids that regulate c-maf expression by increasing its proteasomal degradation through up-regulation of ubiquitin. *Blood.* 2007;110(12):4047–4054.
15. Zavareh RB, Lau KS, Hurren R, et al. Inhibition of the sodium/potassium ATPase impairs N-glycan expression and function. *Cancer Res.* 2008;68(16):6688–6697.
16. Sprangers R, Kay LE. Quantitative dynamics and binding studies of the 20S proteasome by NMR. *Nature.* 2007;445(7128):618–622.
17. Goto NK, Gardner KH, Mueller GA, et al. A robust and cost-effective method for the production of Val, Leu, Ile (delta 1) methyl-protonated 15N-, 13C-, 2H-labeled proteins. *J Biomol NMR.* 1999;13(4):369–374.
18. Kisselev AF, Akopian TN, Woo KM, et al. The sizes of peptides generated from protein by mammalian 26 and 20 S proteasomes. Implications for understanding the degradative mechanism and antigen presentation. *J Biol Chem.* 1999;274(6):3363–3371.
19. Tugarinov V, Hwang PM, Ollerenshaw JE, et al. Cross-correlated relaxation enhanced 1H[bond]13C NMR spectroscopy of methyl groups in very high molecular weight proteins and protein complexes. *J Am Chem Soc.* 2003;125(34):10420–10428.
20. Delaglio F, Grzesiek S, Vuister GW, et al. NMRPipe: a multidimensional spectral processing system based on UNIX pipes. *J Biomol NMR.* 1995;6(3):277–293.
21. Mawji IA, Simpson CD, Hurren R, et al. Critical role for Fas-associated death domain-like interleukin-1-converting enzyme-like inhibitory protein in anoikis resistance and distant tumor formation. *J Natl Cancer Inst.* 2007;99(10):811–822.
22. Al-Nasiry S, Geusens N, Hanssens M, et al. The use of Alamar Blue assay for quantitative analysis of viability, migration and invasion of choriocarcinoma cells. *Hum Reprod.* 2007;22(5):1304–1309.
23. Carter BZ, Gronda M, Wang Z, et al. Small-molecule XIAP inhibitors derepress downstream effector caspases and induce apoptosis of acute myeloid leukemia cells. *Blood.* 2005;105(10):4043–4050.
24. Trudel S, Li ZH, Rauw J, et al. Preclinical studies of the pan-Bcl inhibitor obatoclax (GX015-070) in multiple myeloma. *Blood.* 2007;109(12):5430–5438.
25. Chou TC, Talalay P. Quantitative analysis of dose-effect relationships: the combined effects of multiple drugs or enzyme inhibitors. *Adv Enzyme Regul.* 1984;22:27–55.
26. Zwickl P, Lottspeich F, Dahlmann B, et al. Cloning and sequencing of the gene encoding the large (alpha-) subunit of the proteasome from Thermoplasma acidophilum. *FEBS Lett.* 1991;278(2):217–221.
27. Lowe J, Stock D, Jap B, et al. Crystal structure of the 20S proteasome from the archaeon T. acidophilum at 3.4 A resolution. *Science.* 1995;268(5210):533–539.
28. Sunwoo JB, Chen Z, Dong G, et al. Novel proteasome inhibitor PS-341 inhibits activation of nuclear factor-kappa B, cell survival, tumor growth,

and angiogenesis in squamous cell carcinoma. *Clin Cancer Res.* 2001;7(5):1419–1428.
29. Minderman H, Zhou Y, O'Loughlin KL, et al. Bortezomib activity and in vitro interactions with anthracyclines and cytarabine in acute myeloid leukemia cells are independent of multidrug resistance mechanisms and p53 status. *Cancer Chemother Pharmacol.* 2007;60(2):245–255.
30. Beck WT, Cirtain MC, Look AT, et al. Reversal of Vinca alkaloid resistance but not multiple drug resistance in human leukemic cells by verapamil. *Cancer Res.* 1986;46(2):778–784.
31. van der Heijden J, de Jong MC, Dijkmans BA, et al. Development of sulfasalazine resistance in human T cells induces expression of the multidrug resistance transporter ABCG2 (BCRP) and augmented production of TNFalpha. *Ann Rheum Dis.* 2004;63(2):138–143.
32. van der Heijden J, de Jong MC, Dijkmans BA, et al. Acquired resistance of human T cells to sulfasalazine: stability of the resistant phenotype and sensitivity to non-related DMARDs. *Ann Rheum Dis.* 2004;63(2):131–137.
33. Oerlemans R, van der Heijden J, Vink J, et al. Acquired resistance to chloroquine in human CEM T cells is mediated by multidrug resistance-associated protein 1 and provokes high levels of cross-resistance to glucocorticoids. *Arthritis Rheum.* 2006;54(2):557–568.
34. Cortes J, Thomas D, Koller C, et al. Phase I study of bortezomib in refractory or relapsed acute leukemias. *Clin Cancer Res.* 2004;10(10):3371–3376.
35. Chauhan D, Li G, Shringarpure R, et al. Blockade of Hsp27 overcomes Bortezomib/proteasome inhibitor PS-341 resistance in lymphoma cells. *Cancer Res.* 2003;63(19):6174–6177.
36. Gaczynska M, Osmulski PA, Gao Y, et al. Proline- and arginine-rich peptides constitute a novel class of allosteric inhibitors of proteasome activity. *Biochemistry.* 2003;42(29):8663–8670.

Funding

The Princess Margaret Hospital Foundation; Ontario Institute for Cancer Research through the Ministry of Research and Innovation; Leukemia and Lymphoma Society.

Notes

L. E. Kay is a Canada Research Chair in Biochemistry. A. D. Schimmer is a Leukemia and Lymphoma Scholar in Clinical Research. S. Trudel has received research funding from OrthoBiotech (which markets bortezomib in Canada). X. Li, T. E. Wood, R. Sprangers, X. Mao, X. Wang, H. Adomat, Y. Zhang, S. E. Verbrugge, Z. H. Li, T. L. Religa, and N. E. Franke designed research, analyzed data, performed research, and edited the article. G. Jansen, S. Trudel, H. Messner, J. Cloos, D. R. Rose, R. A. Batey, E. Guns, and L. E. Kay analyzed data and supervised research. C. Chen, N. Jamal, and A. Navon provided critical reagents. A. D. Schimmer designed and supervised the research, analyzed data, and wrote the article. All authors reviewed and edited the article. The study sponsors did not have a role in the study, writing the manuscript, or the decision to submit the manuscript for publication.

Present address: Department of Biology, University of Waterloo, Waterloo, ON, Canada (D. R. Rose).

We thank Dr Doug Kuntz for helpful advice and discussion and Dr Tony Panzarella for statistical advice.

Affiliations of authors: Ontario Cancer Institute, Princess Margaret Hospital, Toronto, ON, Canada (XL, TEW, XM, XW, YZ, ZHL, ST, CC, NJ, HM, DRR, ADS); Department of Chemistry (TEW, YZ, RAB, RS, TLR, LEK), Department of Medical Genetics (RS, TLR, LEK), Department of Biochemistry (RS, TLR, LEK), Department of Medicine (ST, CC, HM, ADS), and Department of Medical Biophysics (ST, HM, DRR, ADS), University of Toronto, Toronto, ON, Canada; Department of Pediatric Oncology and Department of Rheumatology, VU University Medical Centre, Amsterdam, the Netherlands (GJ, NEF, SEV, JC); Prostate Centre at Vancouver General Hospital, Vancouver, BC, Canada (HA, EG); Department of Biological Investigation, Weizmann Institute of Science, Rehovot, Israel (AN); Department of Urologic Sciences, University of British Columbia, Vancouver, BC, Canada (EG).